

Temperature effects on dielectric liquid lenses

Hongxia Zhang,^{1,2} Hongwen Ren,³ Su Xu,² and Shin-Tson Wu^{2,*}

¹The College of Precision Instrument and Opto-electronics Engineering, Tianjin University, Tianjin 300072, China

²CREOL, The College of Optics and Photonics, University of Central Florida, Orlando, Florida 32816, USA

³Dept. of Polymer Nano Science and Tech., Chonbuk National University, Jeonju, Jeonbuk, 561-756, South Korea
swu@ucf.edu

Abstract: The thermal stability of dielectric liquid lenses is studied by measuring the focal length at different temperatures. Two types of liquids lenses are investigated: Type-I (SL-5267/glycerol) and Type-II (glycerol/BK7 matching liquid). A threshold-like behavior is found. Below the threshold temperature, the focal length is temperature insensitive. Above the threshold, the focal length changes exponentially with the temperature. Both refractive index and surface profile are responsible for the focal length change, although the former decreases linearly with the temperature. The threshold temperature of Type-I and Type-II liquid lens are 60°C and 40°C, respectively. Type-I lens shows a good temperature stability in a wide range. Moreover, the lens can recover to its original state even though it is operated at a high temperature.

©2014 Optical Society of America

OCIS codes: (010.1080) Adaptive optics; (220.3630) Lenses; (230.2090) Electro-optical devices.

References and links

1. L. Dong, A. K. Agarwal, D. J. Beebe, and H. R. Jiang, "Adaptive liquid microlenses activated by stimuli-responsive hydrogels," *Nature* **442**(7102), 551–554 (2006).
2. S. Kuiper and B. H. W. Hendriks, "Variable-focus liquid lens for miniature cameras," *Appl. Phys. Lett.* **85**(7), 1128–1130 (2004).
3. C. A. López and A. H. Hirsra, "Fast focusing using a pinned-contact oscillating liquid lens," *Nat. Photonics* **2**(10), 610–613 (2008).
4. G. Zhou, H. M. Leung, H. Yu, A. S. Kumar, and F. S. Chau, "Liquid tunable diffractive/refractive hybrid lens," *Opt. Lett.* **34**(18), 2793–2795 (2009).
5. S. Murali, K. P. Thompson, and J. P. Rolland, "Three-dimensional adaptive microscopy using embedded liquid lens," *Opt. Lett.* **34**(2), 145–147 (2009).
6. B. A. Malouin, Jr., M. J. Vogel, J. D. Olles, L. Cheng, and A. H. Hirsra, "Electromagnetic liquid pistons for capillarity-based pumping," *Lab Chip* **11**(3), 393–397 (2011).
7. H. Ren and S. T. Wu, "Variable-focus liquid lens," *Opt. Express* **15**(10), 5931–5936 (2007).
8. H. Oku and M. Ishikawa, "High-speed liquid lens with 2 ms response and 80.3 nm root-mean-square wavefront error," *Appl. Phys. Lett.* **94**(22), 221108 (2009).
9. U. Zabit, R. Atashkoei, T. Bosch, S. Royo, F. Bony, and A. D. Rakic, "Adaptive self-mixing vibrometer based on a liquid lens," *Opt. Lett.* **35**(8), 1278–1280 (2010).
10. J. K. Lee, K. W. Park, H. R. Kim, and S. H. Kong, "Durability enhancement of a microelectromechanical system-based liquid droplet lens," *Jpn. J. Appl. Phys.* **49**, 06GN11 (2010).
11. S. W. Lee and S. S. Lee, "Focal tunable liquid lens integrated with an electromagnetic actuator," *Appl. Phys. Lett.* **90**(12), 121129 (2007).
12. C. A. López, C. C. Lee, and A. H. Hirsra, "Electrochemically activated adaptive liquid lens," *Appl. Phys. Lett.* **87**(13), 134102 (2005).
13. D. Koyama, R. Isago, and K. Nakamura, "Compact, high-speed variable-focus liquid lens using acoustic radiation force," *Opt. Express* **18**(24), 25158–25169 (2010).
14. J. Y. An, J. H. Hur, S. Kim, and J. H. Lee, "Spherically encapsulated variable liquid lens on coplanar electrodes," *IEEE Photon. Technol. Lett.* **23**(22), 1703–1705 (2011).
15. B. Berge, "Liquid lens technology: principle of electrowetting based lenses and applications to imaging," 18th IEEE International Conference on Micro Electro Mechanical Systems, 227–230 (2005).
16. Y. Park, S. Seo, P. Gruenberg, and J.-H. Lee, "Self-centering effect of a thickness-gradient dielectric of an electrowetting liquid lens," *IEEE Photon. Technol. Lett.* **25**(6), 623–625 (2013).
17. C. U. Murade, J. M. Oh, D. van den Ende, and F. Mugele, "Electrowetting driven optical switch and tunable aperture," *Opt. Express* **19**(16), 15525–15531 (2011).

18. C. C. Cheng and J. A. Yeh, "Dielectrically actuated liquid lens," *Opt. Express* **15**(12), 7140–7145 (2007).
19. H. Ren, H. Xianyu, S. Xu, and S. T. Wu, "Adaptive dielectric liquid lens," *Opt. Express* **16**(19), 14954–14960 (2008).
20. H. Ren, S. Xu, and S. T. Wu, "Deformable liquid droplets for optical beam control," *Opt. Express* **18**(11), 11904–11910 (2010).
21. H. Ren, S. Xu, D. Ren, and S. T. Wu, "Novel optical switch with a reconfigurable dielectric liquid droplet," *Opt. Express* **19**(3), 1985–1990 (2011).
22. H. Ren, S. Xu, Y. Liu, and S. T. Wu, "Electro-optical properties of dielectric liquid microlens," *Opt. Commun.* **284**(8), 2122–2125 (2011).
23. S. Xu, H. Ren, Y. Liu, and S. T. Wu, "Dielectric liquid microlens with switchable negative and positive optical power," *J. MEMS* **20**(1), 297–301 (2011).
24. T. Krupenkin, S. Yang, and P. Mach, "Tunable liquid microlens," *Appl. Phys. Lett.* **82**(3), 316–318 (2003).
25. J. Li, C. H. Wen, S. Gauza, R. B. Lu, and S. T. Wu, "Refractive indices of liquid crystals for display applications," *J. Display Technol.* **1**(1), 51–61 (2005).
26. http://en.wikipedia.org/wiki/Surface_tension.
27. J. D. Bernardin, I. Mudawar, C. B. Walsh, and E. I. Franses, "Contact angle temperature dependence for water droplets on practical aluminum surfaces," *Int. J. Heat Mass Tran.* **40**(5), 1017–1033 (1997).

1. Introduction

Adaptive liquid lenses provide innovative and exciting opportunities to enhance the optical performance, accuracy, throughput, and reliability while reducing overall cost in machine vision, medical, and optical communication systems [1–9]. Various approaches have been proposed to achieve adaptive focus [10–14]. Among them, electrowetting [15–17] and dielectrophoretic effect [18–23] are considered as the most attractive ones in terms of compactness and simple electrical actuation. Unlike an electrowetting lens which employs a conductive liquid (e.g., salty water), dielectrophoretic lens utilizes dielectric liquids. Thus, the lens characteristic can be improved by choosing proper dielectric liquids, which offer better physical properties without the concern of evaporation, microbubbles, and hysteresis.

In a dielectrophoretic lens, two immiscible liquids with different dielectric constants are employed. One liquid forms a droplet on a substrate and the other liquid fills the surrounding, in which the liquid-liquid interface functions as a refractive surface. Under an inhomogeneous electric field, the generated dielectric force can deform the interface. As a result, the focal length can be tuned. Various dielectric liquid lenses have been demonstrated and their characteristics studied [10,11]. Most of them are operated at room temperature rather than an elevated temperature. In practical applications, the ambient temperature may change, which would affect the lens' focal length and imaging performance because the physical properties of the employed liquids are temperature dependent. Therefore, studying the temperature effect on a dielectric liquid lens is critically important for practical applications. Dielectric liquid lenses with a wide range of operating temperature are highly desirable.

In this paper, we prepared two dielectric liquid lenses with two liquid pairs, and evaluated their temperature dependent focal length and image performance. The liquid lens with SL-5267 optical fluid and glycerol presents very good thermal stability as long as the temperature is below 70 °C. It recovers to its original state even heated at 130 °C for several minutes.

2. Device structure and evaluation method

Figure 1(a) depicts the side-view structure of our dielectric liquid lens. The lens chamber consists of two glass substrates. Each substrate has a continuous indium tin oxide (ITO) electrode, followed by a dielectric layer. A small amount of liquid-1 is dripped on the dielectric layer to form a droplet, and liquid-2 fills the surrounding chamber. The cell gap was controlled by a 100- μm -thick Mylar spacer. At room temperature, the liquid-liquid interface is indicated by the solid blue curve in Fig. 1(a). Due to the refractive index difference between liquid-1 and liquid-2, the droplet exhibits a lens characteristic. If the refractive index of liquid-1 is larger than that of liquid-2, then the incident light will be focused. On the other hand, if liquid-1 has a smaller thermal expansion coefficient than liquid-2, then the curvature of the liquid-liquid interface would become flatter as the temperature increases, as shown by

the red dashed lines in Fig. 1(a). As a result, the focal length increases accordingly, which can be monitored by an optical microscope (OM). To study the temperature effect, the fabricated liquid lens was placed in a closed chamber (Linkam, LTS350), whose temperature was controlled by a computer as Fig. 1(b) shows. Firstly, at room temperature the lens position was adjusted vertically to bring the object into focus and a clear image was observed through the lens. Then the temperature of the chamber was gradually increased, and the image characteristic at various temperatures was observed.

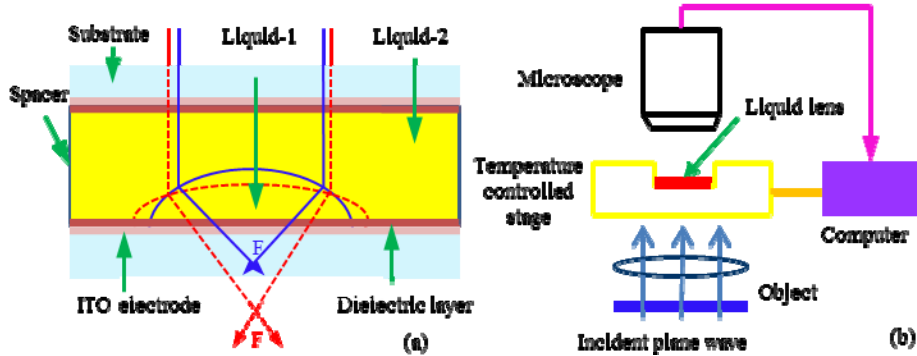


Fig. 1. Dielectric liquid lens structure and experimental setup: (a) side-view of the dielectric liquid droplet lens, and (b) experimental setup for measuring the focal length at various temperatures.

3. Experiment

We fabricated two dielectric liquid lenses with two pairs of liquids: 1) Type-I: optical fluid (SL-5267)/glycerol, and 2) Type-II: BK7 matching liquid/glycerol. Each pair satisfies the following basic requirements: large difference in dielectric constant, large difference in refractive index, and immiscibility. Table 1 lists the physical properties of these three liquids. Although there is a very small density-mismatch in the two liquids (0.01 in Type-I and 0.07 in Type-II), the gravity effect is negligible since the lens is always horizontally placed and the lens droplet is small (only a few microns). However, if the lens is placed vertically, then the gravity effect would be important.

Table 1. Physical Properties of the Three Liquids Employed

Name	Dielectric Constant	Refractive Index	Density(g/cm ³)	Surface tension(dyne/cm)	color
SL-5267	4.7	1.67	1.25	50	clear
Glycerol	47	1.47	1.26	63	clear
BK7 matching liquid	5	1.52	1.33	40	clear

From Table 1, if we use SL-5267 as the droplet and glycerol as the surrounding, the formed lens is a converging lens. The lens aperture is defined as the diameter of the circular contacting area between the droplet and the bottom substrate. Initially, the droplet is in a relaxing state and the interfacial tension satisfies the following relationship:

$$\gamma_{L1,L2} \cos \theta = \gamma_{L1,S} - \gamma_{L2,S}, \quad (1)$$

where γ is the interfacial tension, subscripts $L1$, $L2$ and S denote liquid-1, liquid-2, and bottom dielectric layer, respectively, and θ is the contact angle between the droplet and the bottom substrate. The focal length of a liquid lens can be approximated as [24]

$$f = \sqrt[3]{\frac{3V_d}{\pi(1 - \cos\theta)(2 - \cos^2\theta - \cos\theta)(n_1 - n_2)^3}}, \quad (2)$$

where V_d is the droplet volume, n_1 and n_2 are the refractive index of liquid-1 and liquid-2, respectively. For different-sized droplets, their surface profiles are different. As a result, their focal lengths are different at room temperature (RT).

4. Results and discussions

We first observed the imaging property of the lens made of SL-5267 and glycerol, designated as Type-I. The lens aperture is $\sim 152 \mu\text{m}$. A letter “A” typed on a transparency was placed under the microscope as an object. Figure 2(a) shows the image taken through the lens at RT $\sim 23^\circ\text{C}$. Such a lens is converging, thus the observed image is inverted. Next, we raised the chamber temperature gradually, and the observed image kept clear. As the temperature reached 70°C , the image became blurry [Fig. 2(b)]. Such a result implies that the focal length of the lens has changed. At this stage, if we slightly adjusted the lens position in vertical direction a clear image could still be restored. As the temperature reached 100°C , the image became more blurry [Fig. 2(c)]. At 130°C , the image was hardly recognized [Fig. 2(d)].

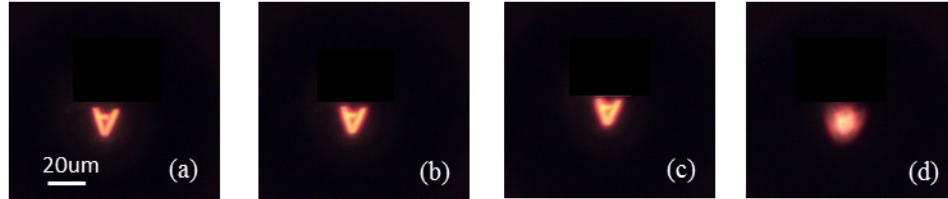


Fig. 2. Image of letter “A” observed through the Type-I liquid lens at various temperatures: (a) 23°C , (b) 70°C , (c) 100°C and (d) 130°C . The diameter of the droplet is $152 \mu\text{m}$.

To quantitatively study the temperature effect, we prepared four microlenses with apertures of $\sim 304 \mu\text{m}$, $\sim 190 \mu\text{m}$, $\sim 170 \mu\text{m}$, and $\sim 35 \mu\text{m}$, respectively. Figure 3 depicts the measured focal length at various temperatures. A voltage was always applied to test the lens at each temperature point before measuring its focal length. The purpose is to ensure the lens is not damaged (i.e. can be actuated by voltage), especially at high operating temperatures. Below 60°C , the focal length of each lens is quite inert to the temperature change. Above 60°C , the focal length of each lens gradually increases, in which the trend can be fitted by the following semi-empirical equation:

$$f = f_0 + Ae^{-T/T_0}, \quad (3)$$

where f_0 , A , T and T_0 are the offset, amplitude, operating temperature and temperature constant of the liquid lens, respectively. The fitting results are shown as solid lines in Fig. 3 and the fitting values listed in Table 2. From Fig. 3, Type-I liquid lens (SL-5267 and glycerol) is temperature insensitive up to 60°C .

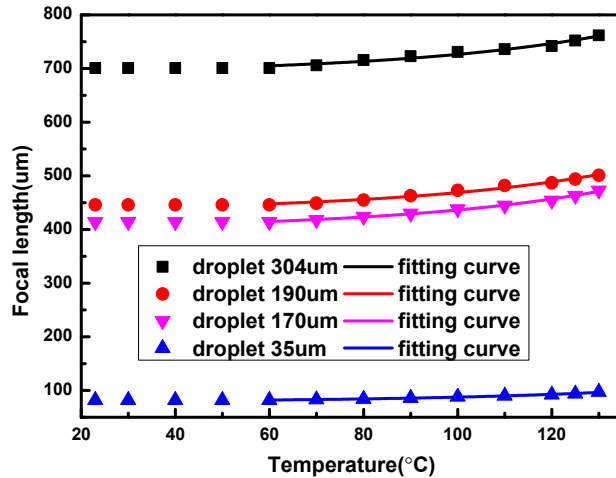


Fig. 3. Focal length of four Type-I liquid lenses measured at various temperatures.

Type-II liquid lens is made of glycerol and BK7 matching liquid, in which glycerol forms a droplet and BK7 matching liquid fills the surrounding. Because the refractive index of glycerol is smaller than that of BK7 matching liquid, the formed liquid lens is a diverging one. The lens aperture is $\sim 85 \mu\text{m}$. The imaging performance of the lens is evaluated by the same method shown in Fig. 2. Through the diverging liquid lens, an upright image of letter “A” is observed, as shown in Fig. 4. At room temperature ($\sim 23 \text{ }^\circ\text{C}$), the observed image is clear [Fig. 4(a)]. At $50 \text{ }^\circ\text{C}$, the image becomes blurry [Fig. 4(b)]. At $70 \text{ }^\circ\text{C}$, the image becomes more blurry [Fig. 4(c)]. At $100 \text{ }^\circ\text{C}$, the image is difficult to recognize [Fig. 4(d)]. These results imply that the focal length of this lens is sensitive to the temperature increase.

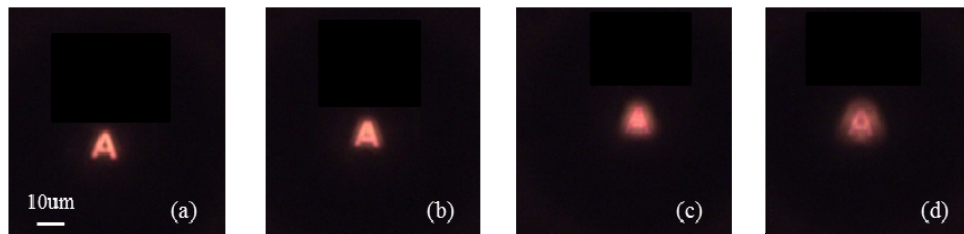


Fig. 4. Image of letter “A” observed through the Type-2 liquid lens at various temperatures: (a) $23 \text{ }^\circ\text{C}$, (b) $50 \text{ }^\circ\text{C}$, (c) $70 \text{ }^\circ\text{C}$, and (d) $100 \text{ }^\circ\text{C}$. The diameter of the glycerol droplet is $85 \mu\text{m}$.

Figure 5 shows the measured focal length of two Type-II liquid lenses at various temperatures. The lens apertures are $\sim 85 \mu\text{m}$ and $\sim 47 \mu\text{m}$, respectively. Below $50 \text{ }^\circ\text{C}$, their focal length is insensitive to the temperature change. Above $50 \text{ }^\circ\text{C}$, their focal length begins to increase, and the trend can be fitted by Eq. (3). The fittings are presented by the red and black lines in Fig. 5, and the fitting parameters are listed in Table 2.

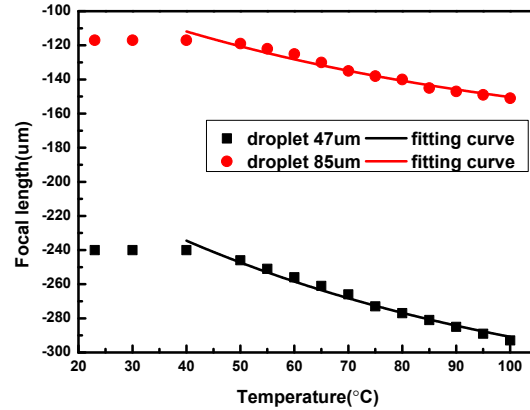


Fig. 5. Temperature dependent focal length of two Type-II liquid lenses.

Table 2. Fitting Parameters f_0 , A and T_0 for Curves Shown in Fig. 3 and Fig. 5

Liquid pair	Droplet diameter (μm)	f_0 (μm)	A (μm)	T_0 ($^\circ\text{C}$)	R-square
Type-I: SL-5267/glycerol	304	690	3.92	-45	0.97
	190	433	3.86	-45	0.98
	170	400	3.97	-45	0.99
	35	78	1.01	-45	0.99
Type-II: glycerol/BK7 matching liquid	85	-337	175	75.6	0.98
	47	-182	119	75.6	0.96

The parameter f_0 mainly depends on the refractive indices of the two employed liquids, droplet diameter, and the initial contact angle. For the liquid lens made of same liquid pair on the same dielectric layer, according to Eq. (1) the initial contact angle should be the same. As expected, the parameter f_0 is linearly proportional to the diameter of the droplets. From the data listed in Table 2, this proportionality constant is estimated to be ~ 2.28 for Type-I liquid lens and ~ 3.92 for Type-II liquid lens. The temperature constant T_0 is determined by the properties of the liquids. For Type-I liquid lens, its temperature constant is negative and smaller compared to that of Type-II.

We also investigated the temperature hysteresis of Type-I liquid lenses. The lens aperture is $304 \mu\text{m}$. Figure 6 shows the measured focal length when the operating temperature increases (red squares) from RT to 130°C and then decreases to RT again (blue dots). These two curves overlap well. Such a result implies that our liquid lens can be safely operated at 130°C since it can return to the initial state as the temperature decreases to RT. However, further increasing the temperature will damage the cell. For example, if the temperature exceeds 150°C , the lens characteristic is vanished and the lens can no longer return to its initial state even if the temperature is decreased to RT.

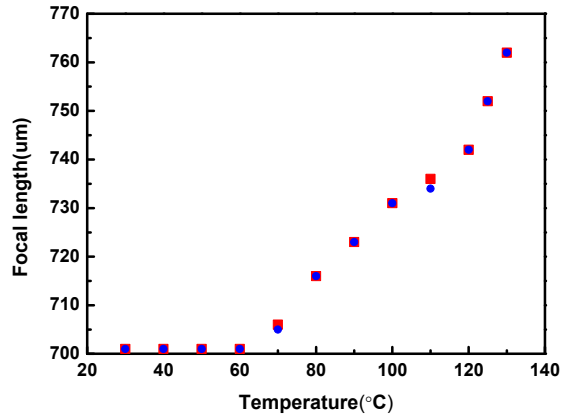


Fig. 6. Temperature hysteresis test of Type-I liquid lens with 304- μm aperture.

Overall speaking, we find that Type-I dielectric liquid lens has a better thermal stability than Type-II. Moreover, the focal length of Type-I liquid lens is temperature insensitive when it is operated below 60 °C. Therefore, SL-5267/glycerol is more favorable for preparing a dielectric liquid lens in terms of thermal stability.

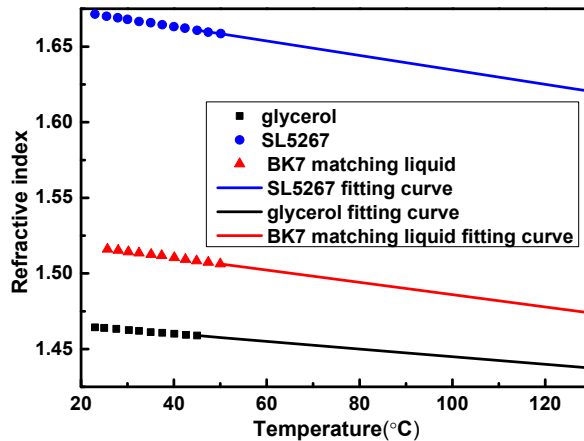


Fig. 7. Refractive index of three liquids versus temperature change.

From Eq. (2), the focal length is mainly determined by the refractive indices of two liquids and the radius of curved interface. To study which factor plays the dominant role as the temperature changes, we used Abbe refractometer (ATAGO DR-M4) to measure the refractive index of optical fluid (SL-5267), glycerol and BK7 matching liquid. Results are shown in Fig. 7. The refractive index of these three fluids decreases almost linearly as the temperature increases, similar to liquid crystals and polymers because of the density effect [25]. The operating temperature of our Abbe refractometer is limited to 50 °C. To obtain the refractive index at higher temperatures, we extrapolate the linear curves, as indicated by the solid lines in Fig. 7. The thermal coefficient of the refractive index of optical oil (SL-5267), glycerol, and BK7 matching liquid is $-2.529 \times 10^{-4}/^{\circ}\text{C}$, $-4.772 \times 10^{-4}/^{\circ}\text{C}$ and $-4.07 \times 10^{-4}/^{\circ}\text{C}$, respectively.

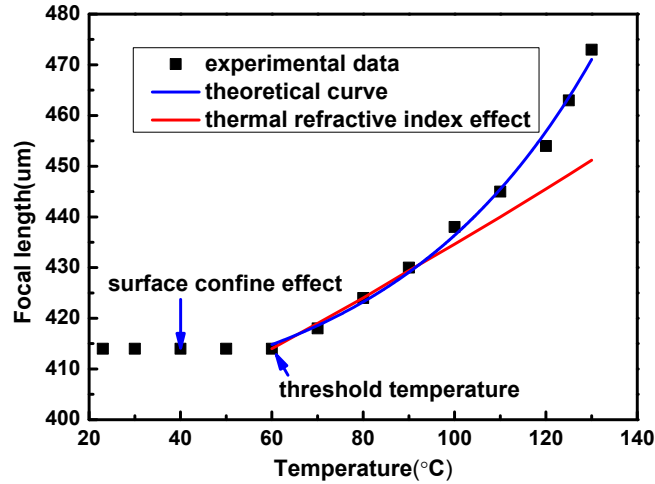


Fig. 8. Focal length vs. temperature.

Figure 8 depicts the temperature dependent focal length of a Type-I liquid lens with 170- μm aperture. From Figs. 3, 5, 6 and 8, one can see that when the temperature increases, the focal length shows a threshold-like behavior. Below the threshold temperature (T_{th}), the focal length is almost inert to the temperature variation. Two possible reasons: (1) From Eq. (1), the liquid-liquid interface (i.e., lens profile) is primarily determined by the surface tension, which is temperature dependent, as expressed by the empirical equation $\gamma V^{2/3} = m(T_c - T)$ [26]. Here V is the molar volume of a substance, T_c is the critical temperature and m is a constant. When the temperature is not very high, the interfacial tensions will not decrease noticeably and the interface almost remains; (2) Due to the surface confinement effect (the lens cell is rigid), the density of the liquids employed in the lens is hardly changed, which implies that the refractive indices of the liquids are hardly changed. Therefore, the focal length variation is not resolvable.

Once the temperature is high enough, the focal length will start to change. The refractive index is linearly dependent on the temperature, which can be expressed as $n_1 = A_1 + B_1 * T$, $n_2 = A_2 + B_2 * T$, where A_1 , B_1 , A_2 , and B_2 are fitting parameters. Through fitting the data shown in Fig. 7, we found $A_1 = 1.68235$, $B_1 = -4.77199 \times 10^{-4}$, $A_2 = 1.47632$, and $B_2 = -2.52866 \times 10^{-4}$. Above T_{th} , the temperature-dependent focal length can be described by:

$$f = \frac{1}{n_1 - n_2} \sqrt{\frac{3V_d}{\pi(1 - \cos \theta)(2 - \cos^2 \theta - \cos \theta)}} = k_n(T) \times \sqrt{\frac{3V_d}{\pi(1 - \cos \theta)(2 - \cos^2 \theta - \cos \theta)}}, \quad (4)$$

$$k_n(T) = \frac{1}{(A_1 - A_2) + (B_1 - B_2) * T}, \quad (5)$$

where $k_n(T)$ is the thermal coefficient due to the refractive index change with temperature. From Eq. (5), the coefficient $(B_1 - B_2 \sim 10^{-4})$ is very small so that the focal length is nearly linearly dependent on the temperature. However, in Figs. 3 and 5 we can see that above T_{th} the focal length is exponentially dependent on the temperature. This implies that in addition to the refractive index change, the interfacial profile should also change with temperature. To prove this, we take the 170- μm -aperture Type-I liquid lens as an example. Figure 8 shows its measured focal length (the filled squares) and the calculated focal length based on Eq. (3) (blue curve). In this calculation, the refractive indices of SL-5267 and glycerol are read from the extrapolated curves shown in Fig. 7. On the other hand, if we assume only the refractive

index changes with the temperature while the other parameters keep constant, then the Zemax simulated focal length should be nearly linearly increased as the temperature exceeds T_{th} , as indicated by the red curve in Fig. 8. It is obvious that there is a discrepancy between the Zemax calculation (red curve) and theoretical results (blue curve, fitted by Eq. (3)). Therefore, in addition to refractive index change, the liquid-liquid interface (e.g., lens profile) should also change with temperature. In Eq. (1), $\gamma_{L1,L2}$, $\gamma_{L1,S}$ and $\gamma_{L2,S}$ are temperature dependent. Adamson used the Gibbs adsorption isotherm, thermodynamics and molecular interaction model to achieve following equation [27]:

$$\cos \theta = 1 + C(T_{co} - T)^{a/(b-a)}, \quad (6)$$

where T_{co} represents a pseudo-critical temperature or the temperature at which the contact angle goes to zero, C is an integration constant, a and b are temperature-independent constants from a balance of intermolecular forces. This model predicts a general experimental trend of θ with respect to T . From Eq. (6), the contact angle decreases as the temperature increases, which means the interface will become flatter and the radius of the interface will increase. This prediction agrees with the experimental results shown in Fig. 8.

According to the empirical equation $\gamma V^{2/3} = m(T_c - T)$ [26], the surface tension is a linear function of temperature. The surface tension of SL-5267, glycerol and BK 7 matching liquid are 50, 63 and 40 dyne/cm, respectively, and the critical temperature of SL-5267, glycerol and BK7 matching liquid are 400 °C, 290 °C, and 160 °C respectively. When the temperature gets as high as 150 °C, the surface tension of SL-5267 and glycerol will become the same, so the contact angle approaches to zero and the lens no longer possesses any optical power, which agrees with the experimental results.

The liquid lens made of glycerol/ BK7 matching liquid has a lower threshold temperature. A possible explanation is that the $d\gamma/dT$ of BK7 matching liquid is larger than those of the two other liquids. Because the original status of the liquid lens balances the surface tensions, the contact angle is stable. When the temperature increases, the surface tension decreases. But if the overall change of surface tension $\gamma_{L1,L2}$, $\gamma_{L1,S}$ and $\gamma_{L2,S}$ can still form the same contact angle, the liquid lens will keep stable. Therefore, to make a dielectric liquid lens with a better thermal stability, which means a higher threshold temperature, the two employed liquids should have similar $d\gamma/dT$ and the $d\gamma/dT$ value should be as small as possible. From the above analysis, both refractive index and interface profile are jointly responsible for the observed focal length change in the high temperature region.

Below T_{th} , the liquid lens is insensitive to the temperature variation. This threshold temperature is governed by the surface tension of the selected liquids. Therefore, choosing proper liquids could fine-tune the desired threshold temperature. Above threshold temperature, the interface profile and the refractive index of the two liquids both change with the temperature. From our experimental results, we indeed find that temperature can affect the focal length of liquid lenses. By choosing different liquids, the lens' temperature stability is different. In contrast to the glycerol/liquid matching BK7, the lenses made from optical oil (SL-5267) and glycerol can present good thermal stability.

5. Conclusion

We studied the thermal effect on various liquid lenses using two different liquid pairs. We find there is a threshold temperature. Below the threshold temperature, the focal length of the liquid lens is temperature insensitive. Above the threshold temperature, the focal length changes exponentially with the temperature while the focal length change caused by refractive index is linearly with the temperature. In this region, both the refractive index and liquid-liquid interface change with temperature. The threshold temperature of Type-I (SL-5267/glycerol) and Type-II (glycerol/BK7 matching liquid) liquid lens are 60°C and 40°C, respectively. The Type-I lens presents a better thermal stability. In a safe temperature range,

the lens can work well without the concern of thermal damage. By choosing a proper liquid pair, liquid lenses with a desired working temperature range can be prepared, which are promising for optical communications, imaging, target tracking, image surveillance systems, and portable electronic devices.

Acknowledgments

The authors are indebted to J. Sun and Y. Chen for their technical assistance and useful discussions. H. Zhang is funded by China Scholarship Council and National Natural Science Foundation of China under Contract No. 41275146. The University of Central Florida group is indebted to the U.S. Air Force Office of Scientific Research (AFOSR) for partial financial support under contract No. FA95550-09-1-0170.